Draft version January 22, 2024
Typeset using LaTeX default style in AASTeX631

Determining the Mass of the Class 0 Protostar Per-emb-14 via Keplerian Dynamics

Cayden Kirkpatrick,[1] Dominique Segura-Cox,[2] and Stella Offner[2]

[1] *University of Wisconsin-Madison*
2535 Sterling Hall 475 N. Charter Street
Madison, WI 53706-1507, USA
[2] *University of Texas at Austin*
Department of Astronomy 2515 Speedway
Austin, TX 78712-1205, USA

ABSTRACT

Protostars in the earliest phases of star formation, Class 0 protostars, are more difficult to observe than their more evolved counterparts due to the greater amount of infalling material surrounding these objects. As a result, only ∼10 masses of Class 0 protostars have dynamical measurements. Here, we measure the mass of Per-emb-14, a Class 0 protostar in the Perseus molecular cloud by fitting Keplerian rotation curves to $C^{18}O$ (2 - 1) data obtained with ALMA. We derived a central protostellar mass of 0.668 ± 0.01 $M_\odot$. This technique for calculating the mass of Per-emb-14 will be used in an upcoming paper which will report the dynamical masses of 9 additional protostars in the Perseus molecular cloud. This calculated mass of Per-emb-14 can be used in conjunction with the other known masses of Class 0 protostars to study their properties and can also be used for studies focusing specifically on Per-emb-14.

1. INTRODUCTION

Per-emb-14, also known as NGC 1333 IRAS4C, is a protostar located in the Perseus molecular cloud at a distance of ∼ 300 pc (Ortiz-León et al. 2018). Per-emb-14 is a single protostar in the youngest Class 0 phase of star formation (e.g., Tobin et al. 2016). Class 0 protostars are still shrouded within the gas of the molecular cloud from which they formed (Andre et al. 2000). However, the molecular cloud obscures emission from these deeply-embedded protostars and their surrounding rotating disks. Consequently the mass of many of these protostars remain unknown; only ∼10 Class 0 protostellar masses have been measured via modeling the Keplerian dynamics of their disks (e.g., Tobin et al. 2012; Murillo et al. 2013; Harsono et al. 2014; Yen et al. 2015; Ohashi et al. 2023). The main obstacle with measuring dynamical masses of embedded systems is to penetrate through the dense environments surrounding young protostars (Looney et al. 2000) to observe the kinematic properties of the rotating disks, which are typically a few 100 au in scale. Such studies require high-resolution interferometers such as the Atacama Large Millimeter/submillimeter Array (ALMA).

2. METHODOLOGY

To conduct this analysis, data was taken from ALMA observations of Per-emb-14. The observations were carried out from 22 to 24 September 2018. The data were calibrated using the ALMA pipeline with the following calibrators: J0510+1800, J0237+2848 (bandpass and flux) and J0336+3218 (phase). We also performed self-calibration on the line-free dust continuum channels and applied the solutions to the line data (see also Tychoniec et al. 2020). This radio data was then analyzed with CASA (CASA Team et al. 2022) to record relevant features of the protostar.

The $C^{18}O$ (2-1) (219.560354 GHz) and SO (6_5 - 5_4) (219.949433 GHz) emission have a spectral resolution of 0.0417 and 0.0832 km/s, respectively. Rest frequencies are taken from SLAIM (F. J. Lovas, private communication; Remijan et al. 2007). The $C^{18}O$ and SO data were then analyzed to observe the motion of the gas around Per-emb-14 and determine if other phenomena were affecting the $C^{18}O$ and SO emission (i.e., infalling streamers or outflows; Pineda et al. 2020; Stephens et al. 2019). We choose to include channels in our analysis where $C^{18}O$ and SO have flux greater than 4σ near source center, where $\sigma = 5.163$ mJy/beam and 4.194 mJy/beam for $C^{18}O$ and SO, respectively.

We then fit for the protostellar mass, producing position-velocity diagrams of Per-emb-14 with both $C^{18}O$ and SO emission, using the python package pvextractor to specify which one-dimensional cut of the raw ALMA data cube to

be used. The angle of this cut was set using the position angle of Per-emb-14 measured from a Gaussian fit to the continuum emission (16.0 degrees). This cut was then fit using the established upper-envelope method, a technique which fits based on the outermost or "upper" data points from a position velocity diagram which are statistically significant (Seifried et al. 2016). This is also known as the 'edge method' (Ohashi et al. 2023). The criterion for statistical significance was again chosen to be 4σ, which has been tested with synthetic observations of simulations and shown to accurately recover the masses of simulated protostars (Seifried et al. 2016). We use the KeplerFit program to perform this analysis (Bosco et al. 2019). The data points to be included in the subsequent fit were selected by eliminating all data between -120 AU and 120 AU separation from the center which is within one beam, or spatial resolution element, of the data. To define an outer limit for performing the Keplerian fit, data was then excluded at radii larger than where we see a visible knee in the position velocity diagrams (in this case, 660 au, see Figure 1c).

3. RESULTS

Per-emb-14 was shown to exhibit clear Keplerian rotation, enabling the calculation of its mass according the steps above. The process of fitting the position-velocity diagram could have been carried out using either $C^{18}O$ or SO, however $C^{18}O$ was selected to find the final value of the mass, as can be seen by the greater rotation in Figure 1a than Figure 1b, and the better fit of the $C^{18}O$ data than the SO data to a negative half root power curve (Figure 1c and Figure 1d). Using the data from $C^{18}O$, the mass was found to be 0.668 solar masses with a standard deviation from the calculation of 0.01. It was also observed that the position-velocity diagrams for $C^{18}O$ and SO do not perfectly fit the expected Keplerian profile; the position-velocity diagrams would only have emission in two quadrants if the gas were only undergoing Keplerian rotation. A possible explanation for this difference is that infalling gas may be showing up in the ALMA data.

The knowledge of this protostar's mass is especially important considering there are only ∼20 other Class 0 or I protostars with known masses. The infalling gas around Per-emb-14 was also prominent in the results of this study. Future work on this source might focus on fitting not only the Keplerian profile but also an infall profile onto the position-velocity diagram. In fact, the ALMA data for Per-emb-14 was taken alongside data for ten other protostars in the Perseus Molecular Cloud, meaning that further analysis of this data is all that is required to find up to ten more Class 0/I protostellar masses. Research is already underway to find the masses of these protostars with results expected to be published in 2024.

4. ACKNOWLEDGEMENTS

This paper makes use of the following ALMA data: ADS/JAO.ALMA#2017.1.01078.S. ALMA is a partnership of ESO (representing its member states), NSF (USA) and NINS (Japan), together with NRC (Canada), MOST and ASIAA (Taiwan), and KASI (Republic of Korea), in cooperation with the Republic of Chile. The Joint ALMA Observatory is operated by ESO, AUI/NRAO and NAOJ. The National Radio Astronomy Observatory is a facility of the National Science Foundation operated under cooperative agreement by Associated Universities, Inc. This research is made possible by the Texas Astronomy Undergraduate Research Experience for Under-represented Students (TAURUS) program which is funded by the National Science Foundation (NSF), National Aeronautics and Space Administration (NASA), the Research Corporation for Science Advancement (RCSA) under a 2019 Cottrell Scholar Award, the Cox Board of Visitors for the University of Texas' Department of Astronomy and McDonald Observatory, and donors to the 2017 TAURUS HornRaiser campaign. This research is also funded by NSF 1812747 and NSF 2107942, and DSC was supported by NSF AAPF Award #AST-2102405.

REFERENCES

Andre, P., Ward-Thompson, D., & Barsony, M. 2000, Protostars and Planets IV, 59

Bosco, F., Beuther, H., Ahmadi, A., et al. 2019, A&A, 629, A10, doi: 10.1051/0004-6361/201935318

CASA Team, Bean, B., Bhatnagar, S., et al. 2022, PASP, 134, 114501, doi: 10.1088/1538-3873/ac9642

Harsono, D., Jørgensen, J. K., van Dishoeck, E. F., et al. 2014, A&A, 562, A77, doi: 10.1051/0004-6361/201322646

Looney, L. W., Mundy, L. G., & Welch, W. J. 2000, ApJ, 529, 477, doi: 10.1086/308239

Murillo, N. M., Lai, S.-P., Bruderer, S., Harsono, D., & van Dishoeck, E. F. 2013, A&A, 560, A103, doi: 10.1051/0004-6361/201322537

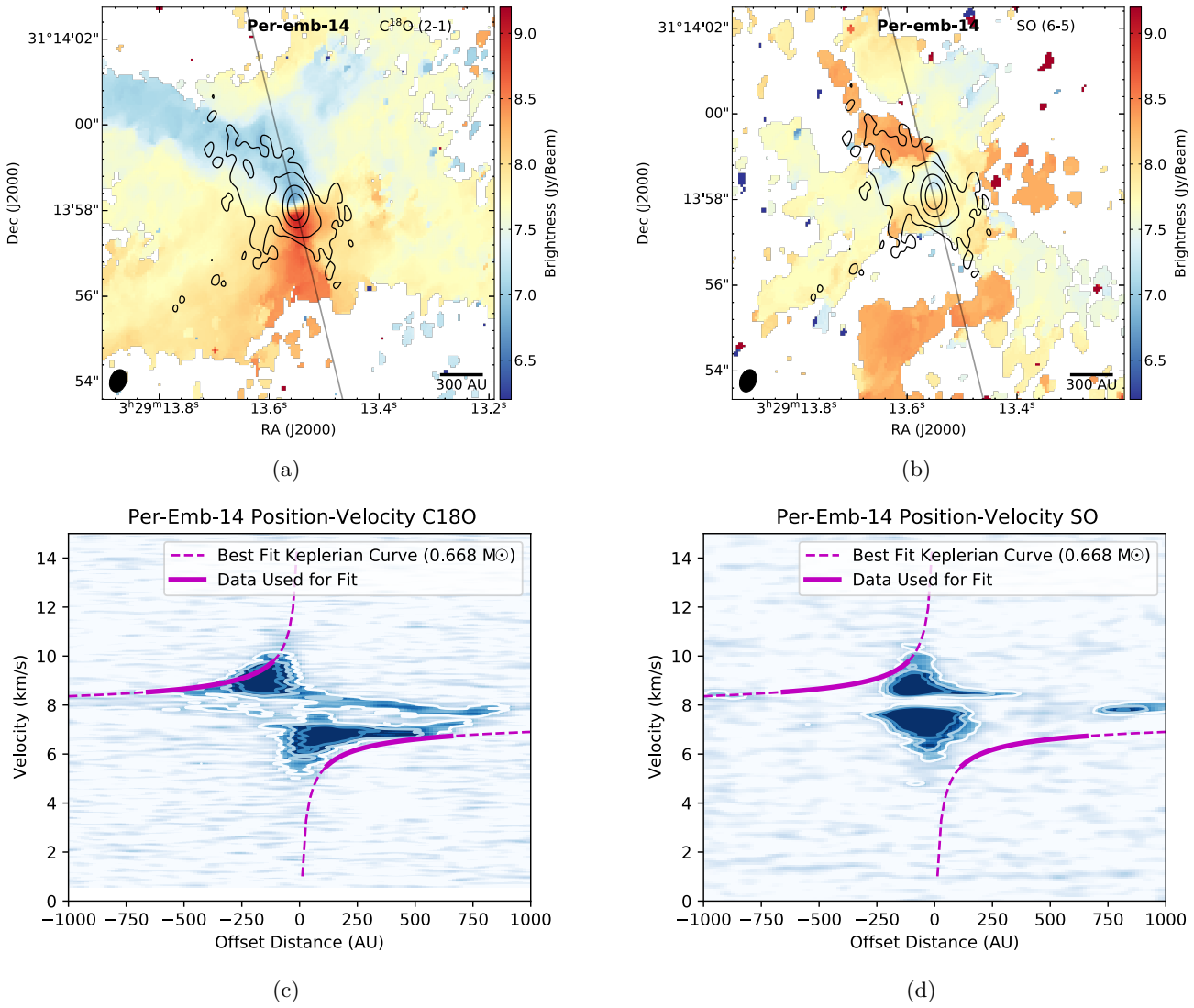

Figure 1: The kinematics of $C^{18}O$ and SO gas around Per-emb-14. (a) Moment 1 map of $C^{18}O$ emission (6.2 km/s to 9.2 km/s). Notice the clear rotation of the protostellar disk indicated by the red and blue regions near the center of the image. (b) Moment 1 map of SO emission (6.2 km/s to 9.2 km/s). The black contours in panels a and b show the continuum emission with levels of 4, 12, 100, and 400σ, where $\sigma = 0.000045$ Jy/beam. (c) Position-velocity diagram of $C^{18}O$ along the cut displayed in panel a. Countours are 4, 8, and 12 σ, where $\sigma = 0.0052$ Jy/beam. (d) Position-velocity diagram of SO along the cut displayed in panel b. Contours are 4, 8, and 12 σ, where $\sigma = 0.0042$ Jy/beam.

Ohashi, N., Tobin, J. J., Jørgensen, J. K., et al. 2023, ApJ, 951, 8, doi: 10.3847/1538-4357/acd384

Ortiz-León, G. N., Loinard, L., Dzib, S. A., et al. 2018, ApJL, 869, L33, doi: 10.3847/2041-8213/aaf6ad

Pineda, J. E., Segura-Cox, D., Caselli, P., et al. 2020, Nature Astronomy, 4, 1158, doi: 10.1038/s41550-020-1150-z

Remijan, A. J., Markwick-Kemper, A., & ALMA Working Group on Spectral Line Frequencies. 2007, in American Astronomical Society Meeting Abstracts, Vol. 211, American Astronomical Society Meeting Abstracts, 132.11

Seifried, D., Sánchez-Monge, Á., Walch, S., & Banerjee, R. 2016, MNRAS, 459, 1892, doi: 10.1093/mnras/stw785

Stephens, I. W., Bourke, T. L., Dunham, M. M., et al. 2019, ApJS, 245, 21, doi: 10.3847/1538-4365/ab5181

Tobin, J. J., Hartmann, L., Chiang, H.-F., et al. 2012, Nature, 492, 83, doi: 10.1038/nature11610
Tobin, J. J., Looney, L. W., Li, Z.-Y., et al. 2016, ApJ, 818, 73, doi: 10.3847/0004-637X/818/1/73
Tychoniec, Ł., Manara, C. F., Rosotti, G. P., et al. 2020, A&A, 640, A19, doi: 10.1051/0004-6361/202037851
Yen, H.-W., Koch, P. M., Takakuwa, S., et al. 2015, ApJ, 799, 193, doi: 10.1088/0004-637X/799/2/193